

Synergetic effect of Mn, Ce, Ba, and B modification and moderate desilication of nanostructured HZSM-5 catalyst on conversion of methanol to propylene

Fateme YAHYAZADEH SARAVI¹, Majid TAGHIZADEH*¹

Department of Chemical Engineering, Babol Noshirvani University of Technology, Babol, Iran

Received: 13.04.2018

Accepted/Published Online: 24.07.2018

Final Version: 06.12.2018

Abstract: Modified mesoporous HZSM-5 catalysts were prepared by controlled desilication using a mixture of NaOH and TPAOH (tetrapropylammonium hydroxide) and impregnation of metals (Mn, Ce, and Ba) and metalloid B. The catalytic performances of all prepared catalysts for methanol to propylene (MTP) reaction were evaluated in a fixed bed reactor under atmospheric pressure at 480 °C. The parent and modified catalysts were characterized by XRD, ICP-OES, FE-SEM, NH₃-TPD, FT-IR, BET, and TGA techniques. The catalyst loaded with 2 wt.% manganese on desilicated HZSM-5 demonstrated the best catalytic performance in terms of the highest selectivity of C₂⁺ to C₄⁺ olefins (about 93%) and about 52% selectivity of propylene at near 99% methanol conversion in the MTP reaction for a long operation (264 h). The improved catalytic performance can be attributed to the high surface area and the formation of mesopores on the zeolite crystals in conjunction with the appropriate acidity.

Key words: Nanostructured ZSM-5, mesoporous, methanol to propylene, desilication, impregnation

1. Introduction

Propylene, the main feedstock for the production of important polymers (e.g., polypropylene), intermediates, and chemicals, can be produced mostly as a byproduct in fluidized catalytic cracking and steam cracking processes. These processes are highly energy-consuming with low olefin yields.¹ The growing demand for propylene and the shortage of petroleum resources resulted in substantial scientific research to achieve a process with higher propylene yield and lower oil dependency.^{2,3} Since methanol can be easily produced from coal and natural gas, which are more accessible than oil resources, the conversion of methanol to propylene (MTP) is a promising method that can be used for petroleum-independent production of propylene.^{4,5} On account of the increasing market demand for propylene rather than ethylene, MTP is more interesting than the methanol to olefin (MTO) reaction.⁶

It is well established that the acidic zeolite catalyst is widely used for the conversion of methanol to hydrocarbons (MTH).⁷ The type of catalyst plays an important role in the product distribution of MTH reactions. Different catalysts are investigated for MTP reactions, including aluminosilicate zeolites such as ZSM-5, ZSM-11, and ZSM-48. However, MTP technology is focused on the development of catalysts with high propylene selectivity, especially high-silica HZSM-5 zeolite.^{8,9} HZSM-5 zeolite is often used as a shape-selective catalyst due to MFI topology and the presence of medium-sized pores (0.5–0.6 nm). Nevertheless, diffusion limitations in microporous zeolite are so severe that they result in mass transfer difficulty and catalyst

*Correspondence: taghizadeh@nit.ac.ir

deactivation (often due to coke deposition on active sites).^{5,10} The generation of mesopores (2–50 nm) in a microporous HZSM-5 catalyst leads to an increment of catalyst lifetime and ease of physical transport.^{11,12}

Different procedures are proposed for the synthesis of hierarchical zeolites, notably with ZSM-5, including: i) use of secondary templates for production of mesopores with primary zeolite template,^{12–14} ii) applying a single multifunctional template that simultaneously produces micropores and mesopores,¹⁵ iii) altering synthesis conditions without applying a secondary template,¹⁶ and iv) defect creation in the crystalline lattice of microporous zeolite by use of leaching reactions such as dealumination^{17,18} and desilication.^{10,19} Although the desilication of ZSM-5 zeolite in alkaline medium (typically NaOH) has been demonstrated as the most promising treatment in terms of simplicity, versatility, and efficiency, the main drawback of this procedure is the uncontrolled silicon extraction, which results in the damage of a significant portion of the zeolite structure.²⁰ As an efficient alkaline treatment for introducing intracrystalline mesopores in zeolites with a high Si/Al ratio or even in the case of pure silica zeolitic materials, the incorporation of a structure-directing agent such as tetraalkylammonium cations in combination with NaOH has been proposed to overcome this problem.¹⁰

Ahmadpour and Taghizadeh¹⁰ studied the effect of high-silica HZSM-5 mesoporosity on the catalytic performance of MTP reaction and their results confirmed that alkaline treatment in a 0.2 M mixture of NaOH/TPAOH solution with TPAOH/(NaOH + TPAOH) = 0.4 led to the highest propylene selectivity (47.21%) and a propylene to ethylene (P/E) ratio of 4.96. The reduction of the diffusion path, the improvement of reactants' accessibility to reactive sites, and the reduction of acid sites' strength without changing the inherent acidity of high-silica ZSM-5 were thought to be the reasons for a better catalytic performance of the desilicated catalyst than the nondesilicated one.²¹ Mei et al¹¹ prepared mesoporous high-silica HZSM-5 by an alkaline desilication treatment (with Na₂CO₃) and a soft template method. The former modification led to an improvement in propylene selectivity up to 42% as well as an increase in the P/E ratio to 10:1, while the latter modification resulted in enhanced propylene selectivity up to 38.8% with P/E ratio of 3.91 in the catalytic conversion of methanol to propylene.

It should be mentioned that the acidity of catalysts has a significant effect on MTP reaction and that the number and strength of acid sites affect methanol conversion and product distribution.^{22,23} Modification of catalysts by metal or metal oxide as promoters is an effective procedure for adjusting the acidity of the HZSM-5.²⁴

Numerous studies have evaluated catalyst promoters for MTP reaction and the results indicated that the yield of propylene was improved by incorporating metal species such as Mn,^{25,26} Fe,⁸ Ca,^{25,27} Ce,^{8,25} Ba,²⁸, and Cs²⁶ into the HZSM-5 catalyst. The results confirmed that even doping of a trace amount of the metal species to the HZSM-5 catalyst could significantly affect the MTP production.²⁹

Similarly, the influence of boron incorporation on HZSM-5 framework in MTP reaction was investigated by some researchers.^{30,31} They concluded that B modification led to increased propylene and light olefin selectivity as well as significant improvement in conversion stability. Liu et al⁸ investigated the effect of some promoters like P, Ce, W, Mn, Fe, Cr, Mo, Ga, V, and Ni on HZSM-5 catalyst with Si/Al = 220 and found that the selectivity of propylene can be improved in the order of P > Ce > W > Mn > Fe > Cr, while Mo, Ga, V, and Ni showed no positive effect on propylene selectivity.

The effect of Zn impregnation on mesoporous ZSM-5 (Si/Al = 26) during the conversion of methanol to gasoline was studied by Ni et al.³² They concluded that catalytic lifetime and aromatics' selectivity were improved compared to unmodified ZSM-5 catalyst. In addition, Ding et al³³ assessed the desilication with a

phosphorous modification of high-silica HZSM-5 in a hydrocarbon cracking process and found that the reduction of diffusion limitation and acidity stabilization resulted in the highest conversion in the bulky molecule cracking reaction.

Despite satisfactory results in the application of H-ZSM-5 zeolite in MTO reaction, much more in-depth investigations are still needed to meet recent challenges, including the optimal acid characteristic in MTP reaction, the most favorable modified element, and further enhancement of the catalytic performance as well as the improvement of catalytic stability and selectivity of the main product.

To our knowledge, there is no report on the assessment of the simultaneous influence of metal/metalloid modification and desilication of high-silica HZSM-5 catalyst in the MTP reaction in the available literature. Therefore, here for the first time the effect of different promoters into desilicated ZSM-5 catalyst on propylene selectivity has been studied in the MTP process. The parent, high-silica HZSM-5 catalyst (Si/Al = 200), was synthesized by a hydrothermal technique, and then mesoporosity was introduced into the parent catalyst by controlled alkaline desilication to decrease the diffusion restriction. In addition, a different amount (0.5, 1, 1.5, 2, 2.5 wt.%) of Mn, Ce, Ba, and B promoters were impregnated on the parent catalyst and all were tested in MTP reactions to find the optimal amount of each promoter to achieve maximum propylene selectivity. These optimal amounts of each promoter on the parent catalyst were chosen for impregnation on the desilicated catalyst. Therefore, the mesoporous desilicated catalysts were modified by a specified percentage of metal/metalloid species as promoters to adjust the acidity of desilicated zeolite. This resulted in a synergy effect of desilication with a metal/metalloid modification. All the catalysts were evaluated in an isothermal fixed bed reactor under atmospheric pressure and at 480 °C.

2. Results and discussion

2.1. Catalyst characterization

2.1.1. XRD analysis

The X-ray diffraction (XRD) patterns of the calcined samples (HZSM-5, DZSM-5, n_{opt} % Me-ZSM-5, and n_{opt} % Me-DZSM-5) are illustrated in Figure 1. All these patterns are in agreement with the typical pattern for the ZSM-5 crystal structure (distinct sharp diffraction peaks in 7–10° and 22.5–25° of the 2θ range) with no extra unidentified phase (before and after modification). It should be noted that no diffraction peaks assigned to metal/metalloid or metal/metalloid oxide clusters were observed in Figure 1. The absence of extra peaks indicates the nanometric size of promoter species and the uniform dispersion thereof (i.e. oxides of promoters) through the ZSM-5 structure. The XRD patterns seem to be identical, and no significant change or damage to the catalyst frameworks occurred in the modification process and calcination. The modified catalysts represent high crystallinity as well as that of the parent (Table 1). After modification, the peak area and intensity decreased slightly, which leads to a slight decline in the relative crystallinity of modified catalysts compared to that of the parent catalyst. As shown in Figure 1a, the intensity of characteristic peaks around $2\theta = 7\text{--}8^\circ$ decreased slightly for the modified catalyst and this reduction can be associated with the presence of metal species in the pore channels of the zeolite.²⁴ The MFI structure of modified ZSM-5 zeolite is protected after desilication and metal/metalloid modification integrated desilication methods (Figure 1b). The slight change in the crystallinity of desilicated ZSM-5 can be attributed to the fact that the material with low crystallites and amorphous phase in the parent HZSM-5 sample is eliminated by alkaline solutions without significant damage of the MFI zeolite framework.¹⁰

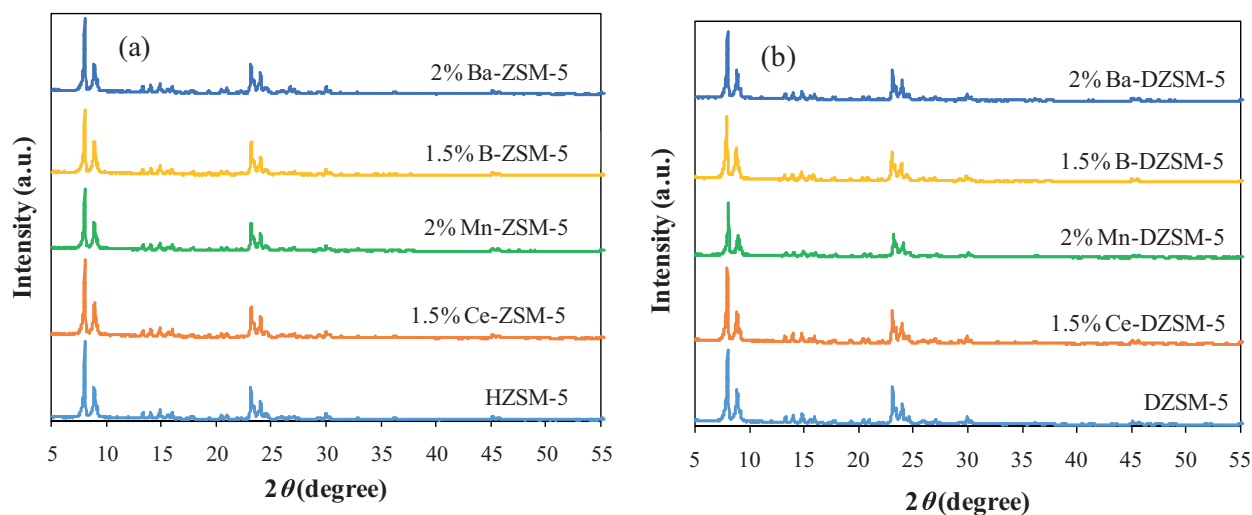


Figure 1. XRD patterns of various catalyst samples: (a) n_{opt} % Me-HZSM-5 and (b) n_{opt} % Me-DZSM-5.

Table 1. Crystallinity, crystal size, and elemental analysis of selected catalyst samples.

Catalyst	Crystallinity (%)	Crystal size (nm)	Metal content ^a (wt.%)	Si/Al ratio ^a
HZSM-5	100	38.9	–	190
2% Mn-ZSM-5	91	36.2	2.10	187
2% Ba-ZSM-5	93	37.2	1.89	188
DZSM-5	95	36.2	–	169
2% Mn-DZSM-5	87	33.6	1.93	167
2% Ba-DZSM-5	90	34.5	2.08	164

^aCalculated by ICP.

It was reported that the alkaline treatment of high-silica zeolite with a pure inorganic alkali (i.e. NaOH) causes excessive desilication.¹⁰ In this method, the silicon and aluminum atoms of the zeolite lattice are extracted and dissolved in the aqueous alkaline phase. Due to the low concentration of Al in the framework of high-silica ZSM-5 (Si/Al = 200), the negative charge of the AlO_4^- tetrahedral only prevents the extraction of Al through hydrolysis of Si – O – Al bonds by hydroxyl anions, while the Si – O – Si bond easily hydrolyzes and the negative charge of AlO_4^- cannot protect neighboring Si atoms from the OH attack. This may lead to a wide extraction of silicon from the zeolite framework. The destruction of a portion of zeolite structure and drastic reduction in XRD peaks' intensity of the NaOH-desilicated HZSM-5 catalyst were reported by some research groups.^{20,34} However, the presence of an organic alkaline like TPAOH in an alkaline solution has a protective effect on the zeolite structure due to the tendency of TPA^+ cations on the zeolite surface. These cations could occupy the pore mouth of porous ZSM-5 and thus protect the structure of zeolite against excessive silicon extraction.^{20,34} Thus, both XRD peaks' intensity and crystallinity of desilicated ZSM-5 (with TPAOH/NaOH treatment) do not significantly change. The relative crystallinity of DZSM-5 is 95%, indicating that the MFI structure of DZSM-5 was well preserved during controlled desilication using the mixture of NaOH and TPAOH.¹⁰ It was reported that after adding a different amount of TPAOH to NaOH solution, the XRD peak intensity of treated samples gradually increased with increasing concentration of TPAOH in TPAOH/NaOH solution. In particular, when HZSM-5 catalyst is desilicated with only TPAOH solution, the intensity of XRD peaks of the modified

catalyst is similar to that of the parent. This can demonstrate the protective effect of TPA^+ cations during the desilication procedure.³⁵

As shown in Figure 1b, the impregnation of the desilicated catalyst with promoters led to more reduction in peak intensity compared with the impregnation of these promoters on the parent catalyst. Therefore, the crystallinity of the Me-DZSM-5 catalyst was slightly lower than that of the other samples.³³ This may be due to the synergetic effect of impregnation and desilication after the integrated modification. The mean diameter of the catalyst crystallites was calculated from the X-ray line broadening according to the Scherrer equation. As can be seen in Table 1, the crystal size of the modified catalyst was not significantly changed.

2.1.2. ICP-OES analysis

As presented in Table 1, the elemental analysis of the selected samples indicates that the measured values of metal content are close to the nominal one, suggesting proper metal impregnation on the parent and desilicated catalysts. Similarly, the bulk Si/Al molar ratio of the catalysts is quantified by ICP-OES. As expected, the results showed that the Si/Al ratio of the DZSM-5 catalyst was reduced compared to that of parent HZSM-5, although the DZSM-5 catalyst still had a high Si/Al ratio of 169, which can be attributed to the mild desilication. Furthermore, the metal impregnation into the parent and DZSM-5 catalysts had a slight effect on this ratio (indeed, the framework and extra-framework species are unable to be distinguished by ICP-OES).

2.1.3. FE-SEM analysis

The surface morphology and structure characteristics of representative samples were evaluated by FE-SEM. As shown in Figure 2, the particles of all the samples had a spherical morphology³⁶ with an identical average particle size of about 2 μm in diameter (with an approximately uniform particle size distribution).

As can be seen in Figure 2a, the external surface of the parent HZSM-5 catalyst is smooth and clear. There is no distinct difference between the morphology of 2% Mn-ZSM-5 (Figure 2b) and 2% Ba-ZSM-5 (Figure 2c) and that of typical HZSM-5, while the alkaline treatment causes a significant change in the surface of the parent zeolite. As illustrated in Figure 2d, the external surface morphology of DZSM-5 became rugged and rough, while the zeolite structure was well preserved.¹⁰ It was reported that the presence of TPAOH in an alkaline solution resulted in the zeolite's protection against nonuniform extraction and severe deterioration of the zeolite surface.³⁵

Impregnation of the metal promoter had no significant effect on the surface morphology of DZSM-5, as shown in Figures 2e and 2f. Lack of agglomeration due to low content of promoters, confirmed by the absence of any extra peaks in XRD analysis, indicates that the converted metal oxide from the initial metal nitrate precursor was dispersed well on HZSM-5 and DZSM-5.^{28,37} SEM images at high magnification of the surface showed that the microsized spherical zeolite sample was generated from the aggregation of nanosized crystals.³⁸ It should be noted that the modified procedures showed no significant changes in crystal size distribution and surface morphology, which is in good agreement with XRD results.

2.1.4. Nitrogen adsorption-desorption analysis

The nitrogen adsorption-desorption isotherms of the parent and selected modified ZSM-5 zeolites are illustrated in Figure 3. Based on the IUPAC classification, the usual Langmuir isotherms of type I and IV are observed for zeolite catalysts, ascribed to microporous and mesoporous structures, respectively. All the nanostructured

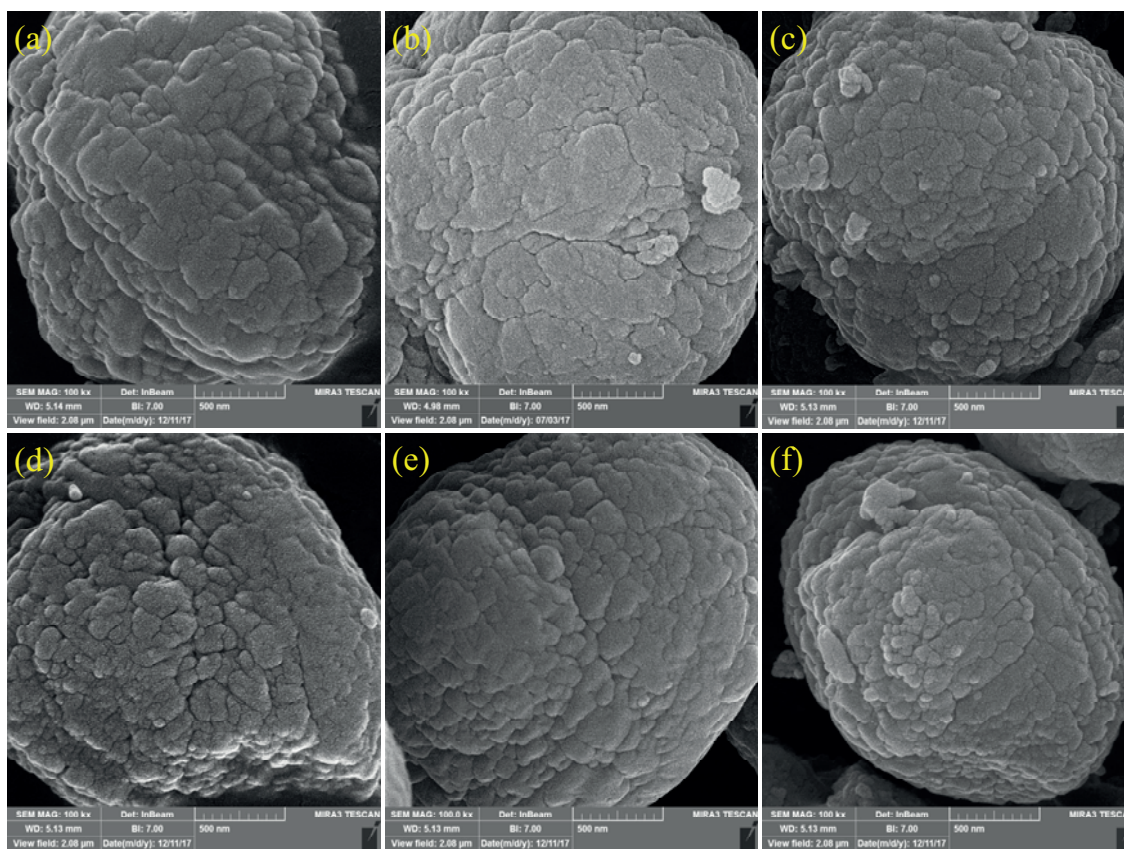


Figure 2. FE-SEM images of the parent and selected modified ZSM-5 samples: (a) HZSM-5, (b) 2% Mn-ZSM-5, (c) 2% Ba-ZSM-5, (d) DZSM-5, (e) 2% Mn-DZSM-5, and (f) 2% Ba-DZSM-5.

samples indicated a type IV isotherm with a hysteresis loop at relative pressures higher than 0.4, representing the existence of both mesopores and micropores in the sample structures. These hysteresis loops are usually attributed to the filling and emptying of mesopores by capillary condensation.^{32,39} According to Figure 3, the N_2 adsorption-desorption isotherms of HZSM-5, 2% Mn-HZSM-5, and 2% Ba-HZSM-5 show minor hysteresis loops compared to those of DZSM-5, 2% Mn-DZSM-5, and 2% Ba-DZSM-5 isotherms with major hysteresis loops. Similarly, the adsorption-desorption branches of Me-DZSM-5 catalysts had a sharper increment at higher P/P_0 , suggesting the presence of larger pores on the zeolite surface of these catalysts.⁴⁰ In addition, the largely parallel arrangement of the adsorption and desorption branches of the hysteresis loop is representative of the presence of cylindrical mesopores connected to the external surface of zeolites.³⁴

The structural properties of selected samples are summarized in Table 2. As expected, the BET surface area and external surface area of DZSM-5 (462.85 and 260.23 $m^2 g^{-1}$, respectively) increased compared to that of the parent catalyst (373.35 and 101.55 $m^2 g^{-1}$). Moreover, the total pore volume increased from 0.184 $mL g^{-1}$ to 0.349 $mL g^{-1}$ and the mesopore volume was enhanced from 0.063 $mL g^{-1}$ to 0.244 $mL g^{-1}$ for HZSM-5 and DZSM-5, respectively. This increment can be attributed to the extraction of Si from the surface and framework of zeolite.

It was reported that desilication of high-silica HZSM-5 with only NaOH solution results in the formation of large-sized of nonuniform mesopores.¹⁰ Conversely, the increasing concentration of TPAOH in NaOH solution

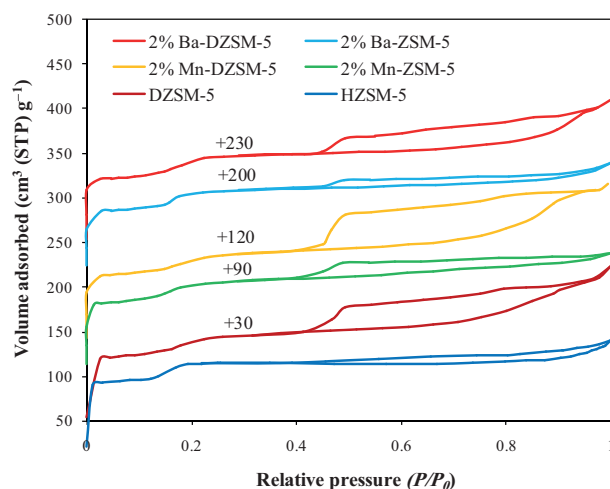


Figure 3. N₂ adsorption-desorption isotherms of the parent and selected modified catalysts.

Table 2. Textural data for selected samples.

Catalyst	S_{total}^a (m ² g ⁻¹)	S_{micro}^b (m ² g ⁻¹)	S_{ext}^c (m ² g ⁻¹)	V_{total}^d (mL g ⁻¹)	V_{micro}^e (mL g ⁻¹)	V_{meso}^f (mL g ⁻¹)	d_{pore}^g (nm)
HZSM-5	373.35	271.80	101.55	0.184	0.121	0.063	1.97
2% Mn-ZSM-5	359.82	250.43	109.39	0.175	0.110	0.065	1.94
2% Ba-ZSM-5	353.78	243.31	107.47	0.171	0.107	0.064	1.93
DZSM-5	462.85	202.62	260.23	0.349	0.105	0.244	3.02
2% Mn-DZSM-5	435.70	193.08	242.62	0.328	0.104	0.224	3.01
2% Ba-DZSM-5	428.72	190.14	238.58	0.321	0.103	0.218	2.99

^aBET surface area.

^b and ^eCalculated using t-plot method.

^cMesopore surface area was evaluated by $S_{total} - S_{micro}$.

^dTotal pore volume at $P/P_0 = 0.99$.

^fMesopore volume was calculated using $V_{total} - V_{micro}$.

^gFrom BET characterization.

leads to the formation of more mesopores with smaller size and further increased external surface area. However, desilication of HZSM-5 with a high concentration of TPAOH and especially only TPAOH solution causes an excessive protective effect. The literature review revealed that the TPA⁺ cations hinder surface desilication by neutralizing the negative charge of the surface. Therefore, the abundant ultrasmall-sized mesopores are formed in zeolite with only TPAOH desilication, which leads to a decrease in external surface area and mesopore volume compared to the zeolite treated with NaOH or a mixture of TPAOH and NaOH solution.³⁵

The BET surface area of 2% Mn-ZSM-5 (359.82 m² g⁻¹) and 2% Mn-DZSM-5 (435.70 m² g⁻¹) decreased slightly compared with that of the parent catalyst and DZSM-5 catalyst, respectively. Similarly, the total pore volume and the micropore volume of the parent catalyst and mesopore DZSM-5 catalyst reduced after Mn modification, which causes some micropore damages or pore blockages due to metal oxide species formation (Me - O).²⁴ The external surface and mesopore volume of 2% Mn-ZSM-5 increasing slightly may be due to partial dealumination during impregnation and the subsequent calcination. Several reports confirmed formation

of mesopores due to dealumination during the impregnation.^{26,41,42} As summarized in Table 2, similar trends are found for 2% Ba-ZSM-5 and 2% Ba-DZSM-5 samples compared to the HZSM-5 and DZSM-5 catalyst, respectively.

Interestingly, the considerable external surface of desilicated ZSM-5 can result in the embedment of a large amount of metal promoters on the surface of zeolite. Since the micropores of the DZSM-5 catalyst are less blocked by the metal promoters, the mesopore zeolite showed a slight reduction of microporous surface and microporous volume after modification with the metal promoter, whereas the mesoporosity of Me-DZSM-5 decreased slightly.³³ As expected, the mean pore diameter of HZSM-5 increased after desilication (from about 1.97 nm to about 3 nm). Furthermore, the pore size decreased slightly after modification by metal promoters, which is possibly due to pore blockage with metal promoters.²⁴

2.1.5. FT-IR analysis

Figure 4 represents the FT-IR spectra of the selected samples. The framework vibrations of zeolites are seen in the region of 400–1400 cm^{-1} (Figure 4a). All of the samples indicate characteristic ZSM-5 structure bonds at 450 cm^{-1} , 550 cm^{-1} , 800 cm^{-1} , 1100 cm^{-1} , and 1225 cm^{-1} . The band appearing at near 450 cm^{-1} can correspond to the T – O (T = Si or Al) bending vibration of the SiO_4 and AlO_4 internal tetrahedral units. The band near 550 cm^{-1} is attributed to the double five-membered ring of ZSM-5 zeolite. The bands at about 800 cm^{-1} and about 1100 cm^{-1} are attributed to the symmetric stretching of the external linkage and internal asymmetric stretching vibration of the Si – O – T linkage, respectively. The absorption at about 1225 cm^{-1} belongs to structures containing four chains of 5-rings resulting in an external asymmetric stretching vibration in ZSM-5 (MFI lattice).^{13,26}

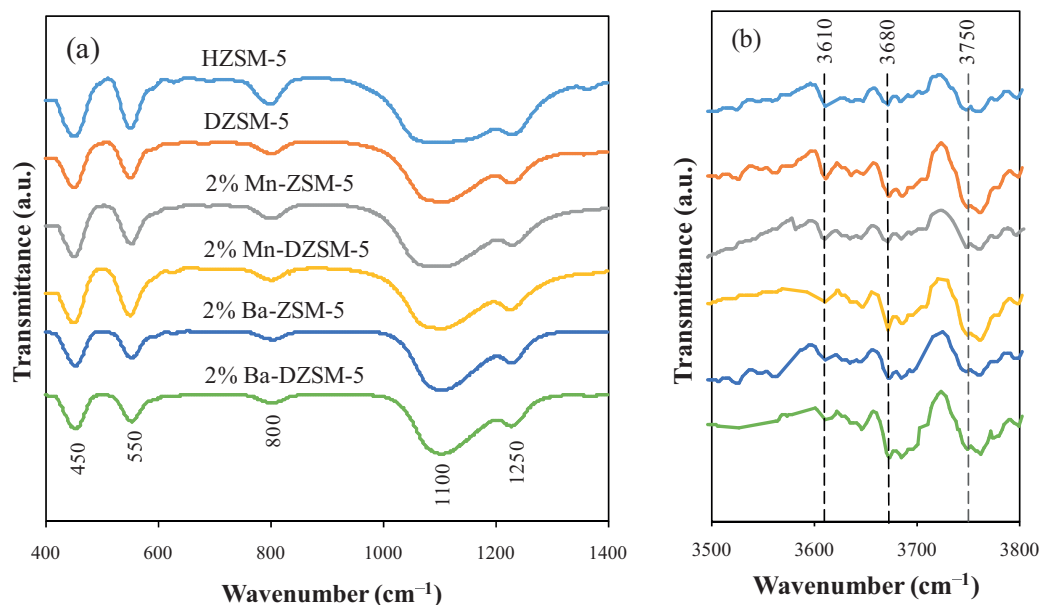


Figure 4. FT-IR spectra of the selected catalysts in the ranges of 400–1400 cm^{-1} (a) and 3500–3800 cm^{-1} (b).

The FT-IR spectra in the region of 3500–3800 cm^{-1} characterize surface hydroxyl (O – H) groups (Figure 4b).⁴³ In this regard, the band at about 3610 cm^{-1} can be assigned to the vibration of bridging Si – (O – H) –

Al group (Brønsted strong acid sites).⁴⁴ The band at about 3680 cm^{-1} can be ascribed to the hydroxyl group linked to extra-framework aluminum species (Al – (O – H)) in the catalyst (Lewis weak acid sites). The band at about 3750 cm^{-1} can be attributed to the lattice terminal Si – O – H (silanol) groups.^{44,45} It was reported that the hydroxyl groups in Si – (O – H) – Al, Al – (O – H), and Si – O – H play a major role in ZSM-5 catalyst acidity.^{26,46}

As can be seen in Figure 4b, the increase in the silanol bond of the desilicated samples (DZSM-5 and M-DZSM-5 catalysts) is in good agreement with the increase of the external surface area of these catalysts. Also, introduction of the promoters into the parent and DZSM-5 catalysts decreases the intensity of the FT-IR bands of Si – OH – Al groups. These results show that the promoter species interact with bridging hydroxyl groups and decrease the Brønsted acid sites.⁴⁷ Furthermore, the bond at 3680 cm^{-1} in FT-IR spectra of the catalysts confirms the extra-framework Al formation.²⁶ It should be noted that the changes in the bonds at about 3610 cm^{-1} and 3680 cm^{-1} are in good accordance with the changes of Brønsted and Lewis acid sites in NH_3 -TPD analysis, respectively.

2.1.6. NH_3 -TPD analysis

The conversion of methanol to propylene is an acidic catalytic reaction that is influenced by the characteristic of acid sites.⁴⁸ The acidity of the catalyst is the most principal factor affecting product distribution and catalyst stability.^{22,23,26} Therefore, the acidity of the selected samples was examined by NH_3 -TPD analysis. Figure 5 shows two desorption peaks at low and high temperatures for selected samples. The temperature of the desorption peak represents the strength of acid sites and the peak area reveals the number (or density) of acid sites. The first peak had a maximum below $300\text{ }^\circ\text{C}$, corresponding to weak Lewis acid sites, while the second peak in the range of $350\text{--}550\text{ }^\circ\text{C}$ was characterized based on the presence of Brønsted strong acid sites in the catalyst. As can be seen in Figure 5, the selected modified catalysts demonstrate a similar pattern of NH_3 -TPD profile compared to HZSM-5, while the peak intensity of weak and strong acid sites were altered considerably. The results of the acid density and the strength of acid sites are represented in Table 3. The parent catalyst contains $0.101\text{ mmol NH}_3\text{ g}^{-1}$ weak and $0.082\text{ mmol NH}_3\text{ g}^{-1}$ strong acid sites. Two desorption peaks of HZSM-5 were observed at $190.2\text{ }^\circ\text{C}$ and $388.1\text{ }^\circ\text{C}$. The slightly higher acidity amount of the DZSM-5 sample (0.109 and 0.095 of $\text{mmol NH}_3\text{ g}^{-1}$ for weak and strong acid sites, respectively) relative to that of the parent may be attributed to realumination during desilication.^{19,33,34}

According to previous reports,^{19,34} some of the framework's aluminum atoms (in addition to silicon atoms) were extracted from the zeolite framework and dissolved in the alkaline solution during desilication. It

Table 3. The NH_3 -TPD data of selected catalyst samples.

Catalyst	Acidity ($\text{mmol NH}_3\text{ g}^{-1}$)				Peak temperature ($^\circ\text{C}$)	
	Weak	Strong	Total	Strong/weak	T_{d1}	T_{d2}
HZSM-5	0.101	0.082	0.183	0.811	190.2	388.1
2% Mn-ZSM-5	0.091	0.061	0.152	0.670	190.1	380.5
2% Ba-ZSM-5	0.112	0.052	0.164	0.464	190	376.3
DZSM-5	0.109	0.095	0.204	0.871	189.5	374.3
2% Mn-DZSM-5	0.117	0.041	0.158	0.350	189.8	370.1
2% Ba-DZSM-5	0.128	0.032	0.16	0.25	189.5	368.7

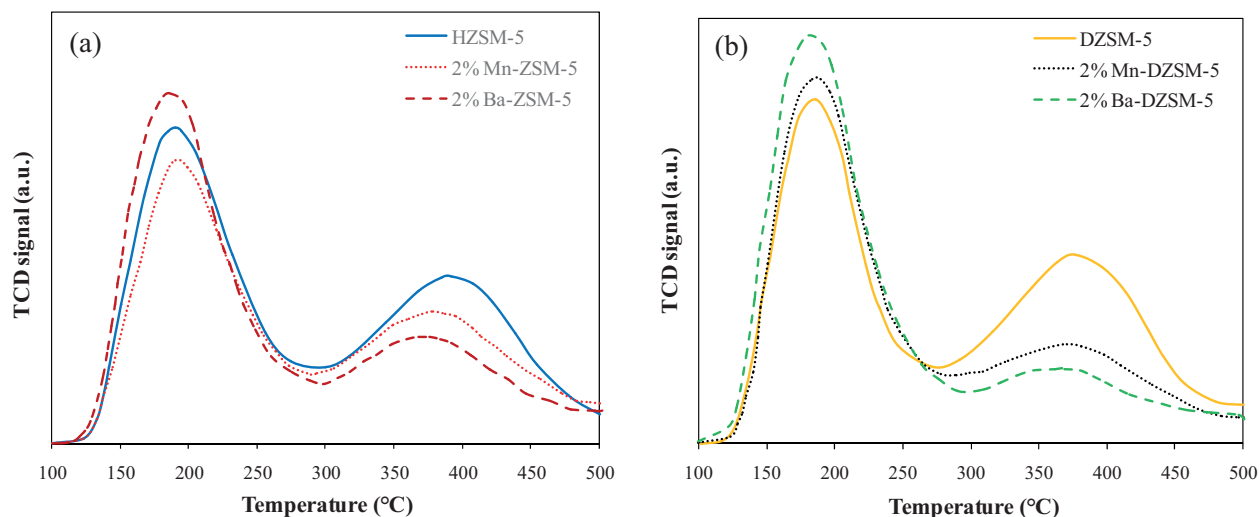


Figure 5. NH_3 -TPD profiles of the modified HZSM-5 (a) and DZSM-5 (b) samples.

cannot be claimed that all the dissolved aluminum during the alkaline treatment remains in the liquid phase, but some is reinserted into tetrahedral framework (realumination). Indeed, when the solution pH decreases due to consumption of OH^- ions during the alkaline treatment, the solubility of Al decreases and then the deposition is accelerated.³⁴

It should be noted that the release of silicon atoms from the structure of zeolite in the alkaline solution increases the number of aluminum atoms per unit mass of zeolite in the framework structure compared to that of parent one.¹⁰ Therefore, the density of strong acid sites of DZSM-5 increases compared to that of the HZSM-5 catalyst. On the other hand, the aluminum atoms deposited on the zeolite framework were dehydroxylated by calcination at 550 °C and turned into extra-framework Al, which led to the increase of Lewis acid site density of the DZSM-5 catalyst compared to that of the parent catalyst.¹⁹

Referring to Figure 5 and Table 3, the high-temperature ammonia desorption peaks shifted to lower temperatures after desilication treatment, indicating a weakening of the strong acid sites' strength of the DZSM-5 catalyst compared to the parent. The reduction of acid site strength may be attributed to the removal of some aluminum atoms in addition to silicon atom extraction from the zeolite framework in alkaline solution.^{19,49}

Also, the impregnation on HZSM-5 catalyst with promoters revealed that the high-temperature desorption peak of Me-ZSM-5 catalysts switched to a relatively lower temperature and the area of this peak was reduced. The results suggest the reduction in the number and strength of strong acid sites as the reduction of total acid site number. Such an alteration in HZSM-5 acidity is in accordance with the results reported in the literature for metal-modified ZSM-5 catalyst.^{24,26,33} It was reported that some metal cations are converted to the corresponding metal oxides during high-temperature calcination and some of them enter the pore channels through a surface thermal diffusion mechanism and lead to promoter interaction with zeolite.⁵⁰ Since each element has a different characteristic and electronegativity, it shows a different interaction with the zeolite lattice. As shown in Figure 5a, the position of the higher desorption peak of 2% Mn-ZSM-5 and 2% Ba-ZSM-5 zeolites shifted to a lower temperature (380.5 °C and 376.3 °C, respectively) compared to that of the parent catalyst (388.1 °C). Additionally, the impregnation of HZSM-5 with Mn reduces the number of weak and strong acid sites as summarized in Table 3. This acidity change observed in the modified ZSM-5 catalyst with other promoters such as P,⁸ Cs,²⁶ and Ce⁵¹ may correspond to the interaction of promoters with the zeolite

framework. The promoters neutralize surface acid sites and also cover the acid sites of zeolite's internal surface with diffusion inside the pores, leading to diminished total density and acid sites' strength of zeolite.^{26,52}

The modification of the parent catalyst with Ba decreases the density of strong acid sites and increases the density of weak acid sites. The production of some Lewis acid sites in the structure of 2% Ba-ZSM-5 may correspond to the combination of promoter species with bridging hydroxyl groups and formation of extra-framework Al.^{53–55} On account of the partial dealumination and formation of new Lewis acid sites, the literature review revealed that impregnation of some promoters such as Mg,²⁶ Mo,^{54,55} B,²³ and Ni⁴⁷ increases the number of Lewis acid sites. This phenomenon can be explained by the interaction of the promoter with the framework Al atoms. In order to provide insight into the nature of the interaction between metal species and HZSM-5 zeolite, some groups evaluated the structure of HZSM-5 after metal impregnation by ²⁷Al MAS NMR technique.^{54,55} They concluded that the metal species can interact with the aluminum atoms and extract some of them from the zeolite framework to form extra-framework Al in high-temperature calcination.

Some studies reported that the partial aluminum extraction from the zeolite framework occurs during the impregnation of the HZSM-5 catalyst with promoters and subsequent calcination.^{26,41,42,56} Despite the partial dealumination during impregnation, it has also been reported that the reduction in number of Lewis acid sites of some modified catalysts may be attributed to the interaction of the promoter with extra-framework Al in addition to framework Al atoms.³³

NH₃-TPD results of Mn and Ba impregnation over desilicated HZSM-5 catalyst are shown in Figure 5b. The results show that when Mn and Ba species are introduced into DZSM-5 by impregnation, the density and strength of strong acid sites of 2% Mn-DZSM-5 and 2% Ba-DZSM-5 catalysts are reduced compared to solo impregnation and desilication, while the density of Lewis acid sites increases compared to solo modification.

Interestingly, the number of Lewis acid sites of the desilicated catalyst increased slightly after Mn impregnation, despite the reduction in Lewis acid site amounts of the parent catalyst after Mn modification. It could possibly be explained by the fact that, after desilication, the reinserted framework aluminum might be less stable than the primary substantial aluminum framework.³³ Hence, during the metal modification and subsequent calcination, it could be omitted from the framework of the desilicated catalyst more easily than the initially instinctive aluminum framework in the HZSM-5 catalyst. Consequently, extra-framework aluminum and subsequently the number of Lewis acid sites increase. Therefore, the strong/weak acid site ratio of Me-DZSM-5 with more extra-framework aluminum was lower than that of DZSM-5 and Me-ZSM-5.

The amount of weak and strong acid sites of nanostructured samples reduced and followed the order of 2% Ba-DZSM-5 > 2% Mn-DZSM-5 > 2% Ba-ZSM-5 > DZSM-5 > HZSM-5 > 2% Mn-ZSM-5 and DZSM-5 > HZSM-5 > 2% Mn-ZSM-5 > 2% Ba-ZSM-5 > 2% Mn-DZSM-5 > 2% Ba-DZSM-5, respectively. Likewise, the strength of strong acid sites weakened in the order HZSM-5 > 2% Mn-ZSM-5 > 2% Ba-ZSM-5 > DZSM-5 > 2% Mn-DZSM-5 > 2% Ba-DZSM-5. It should be mentioned that the strength of the weak acid site did not change significantly after modification, which is consistent with the results reported in other studies.^{10,26}

2.2. Catalytic activity

The catalytic performance of the nanostructured parent and all modified catalysts for the MTP reaction were examined in a fixed bed reactor under the same conditions (T = 480 °C, P = 1 atm, WHSV = 0.9 h⁻¹). Each test was repeated three times and the average value was reported. Since the optimum concentration of promoter mainly affects the catalytic performance of the MTP process and especially propylene selectivity,⁴² first all the HZSM-5 and n% Me-ZSM-5 catalysts with different amounts of promoter loading (n = 0.5, 1,

1.5, 2, 2.5 wt.%) were tested in the fixed bed reactor under the above conditions to find the optimum amount of each promoter (n_{opt} % Me). The results reported in Figure 6 were obtained after 48 h of time on stream (TOS). Propylene selectivity of the parent catalyst was about 34.95% and the loading of different promoters led to various propylene selectivities, while all the modified samples exhibited more propylene selectivity than the parent HZSM-5.

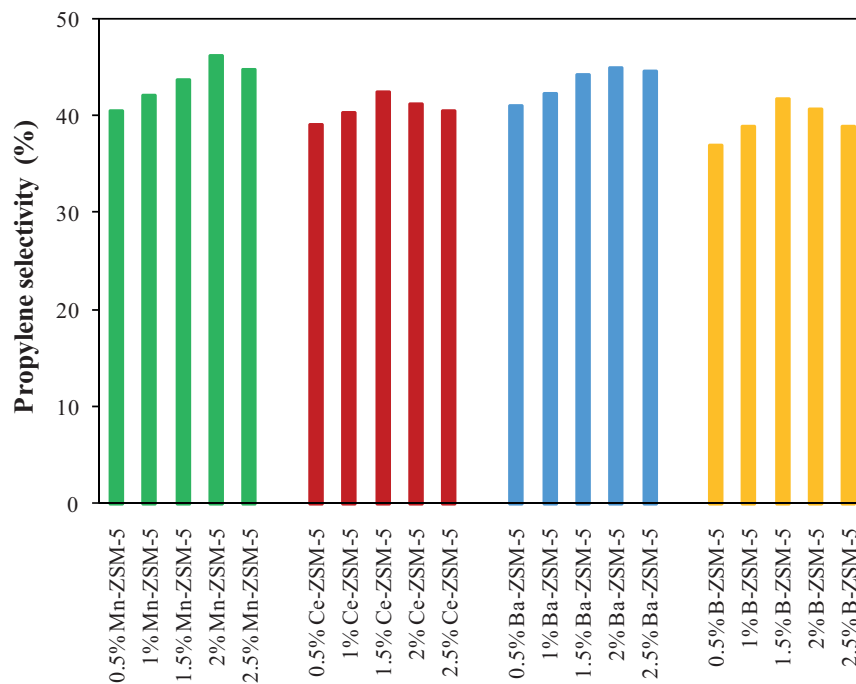


Figure 6. Effect of different contents of promoters on propylene selectivity.

It could be noticed that by loading an appropriate amount of promoters on microporous HZSM-5 greater propylene selectivity was observed. When Mn content increased from 0.5 to 2 wt.%, the propylene selectivity increased from 40.5 to 46.26%. However, the additional loading of Mn on HZSM-5 led to a slight decline in propylene selectivity. Excessive loading of metal may block the pores and channels; the accessibility of reactant molecules to active sites of the catalyst reduces and hence this results in lower selectivity to propylene.⁴² Besides, by increasing Ba content from 0.5 to 2 wt.%, the propylene selectivity was enhanced from 41.14% to 45.09% and then decreased when the content of Ba increased further. Although similar results were observed for cerium and boron as promoters, the difference is that the optimum metal/metalloid content value is 1.5 wt.% and the maximum propylene selectivities are 42.39% and 41.72% for 1.5% Ce-ZSM-5 and 1.5% B-ZSM-5, respectively. The detailed results of n_{opt} % Me-ZSM-5 are summarized in Table 4.

It should be noted that the conversion of n % Me-ZSM-5 catalysts was about 99% at 48 h of TOS. After finding the optimum content of each promoter on microporous HZSM-5, the desilicated catalyst (DZSM-5) was tested in the fixed bed reactor under the aforementioned conditions and then the effects of 2 wt.% Mn, 1.5 wt.% Ce, 2 wt.% Ba, and 1.5 wt.% B on mesoporous DZSM-5 catalyst (n_{opt} % Me-DZSM-5) were examined. The product distributions of the selected catalysts (HZSM-5, DZSM-5, n_{opt} % Me-ZSM-5, and n_{opt} % Me-DZSM-5) are listed in Table 4 after 48 h of TOS. In Table 4, the column of C_1 – C_4 is attributed to light paraffins: methane, ethane, propane, and butane. The columns of C_2^- , C_3^- , and C_4^- are respectively assigned to ethylene,

Table 4. The conversion and product distribution of MTP reaction over catalyst samples after TOS of 48 h.

Catalyst	Conversion	Selectivity						P/E
		C ₁ -C ₄	C ₂ ⁼	C ₃ ⁼	C ₄ ⁼	C ₅ ⁺	C ₂ ⁼ -C ₄ ⁼	
HZSM-5	98.5	4.55	10.91	34.95	21.52	28.07	67.38	3.20
2% Mn-ZSM-5	98.9	3.20	12.12	46.26	28.79	9.63	87.17	3.82
1.5% Ce-ZSM-5	98.8	5.38	11.83	42.39	27.55	12.85	81.77	3.58
2% Ba-ZSM-5	98.9	2.87	7.55	45.09	29.49	15	82.13	5.97
1.5% B-ZSM-5	98.8	5.83	11.16	41.72	26.96	14.33	79.84	3.74
DZSM-5	99.1	3.65	8.91	46.50	29.34	11.6	84.75	5.22
2% Mn-DZSM-5	99.4	3.41	9.39	51.95	32.21	3.04	93.55	5.53
1.5% Ce-DZSM-5	99.4	5.07	12.93	48.85	29.21	3.94	90.99	3.77
2% Ba-DZSM-5	99.4	2.85	8.33	50.05	33.92	4.85	92.30	6.00
1.5% B-DZSM-5	99.3	4.30	11.22	48.51	31.81	4.16	91.54	4.32

propylene, and butylenes. Column C₂⁼-C₄⁼ is attributed to light olefins (sum of C₂⁼, C₃⁼, and C₄⁼). Column C₅⁺ is related to heavy hydrocarbon composed of higher paraffins (>C₄), heavy olefins (>C₄⁼), and aromatics such as benzene, toluene, and xylene (BTX).

As mentioned in Table 4, all modified samples are effective in the MTP reaction under steady operational conditions. As mentioned previously, the parent HZSM-5 catalyst has a good selectivity towards propylene (34.95%) and light olefins (67.38%) and a propylene/ethylene ratio of 3.2 in the MTP reaction.

There is general agreement that a good acidity adjustment containing moderate acid density and no extreme strong acidity is essential for production of highly selective propylene in the MTP reaction.^{5,26} Some groups also reported that the relative amount of weak and strong acid sites has an important effect on MTP reaction.^{22,26} It has been reported that the methanol to DME conversion generally occurs on the Lewis acid sites, whereas the DME (and methanol) to light olefins conversion happens mainly on the Brønsted acid sites.^{5,57}

As previously mentioned, the acidity control of HZSM-5 by modification with different promoters is one of the approaches that improves the catalytic performance of the parent catalyst.²⁶ As can be seen in Table 4, the change in propylene selectivity and product distribution reveals a significant effect of promoters on the HZSM-5 catalytic performance. The results showed that 2% Mn-ZSM-5 and 2% Ba-ZSM-5 with a propylene selectivity of higher than 45% provide better performance compared to those of HZSM-5, 1.5% Ce-ZSM-5, and 1.5% B-ZSM-5. Moreover, 2% Mn-ZSM-5 (about 87%) had the highest light olefin selectivity among all *n_{opt}* % Me-ZSM-5 catalysts, while the light olefin selectivities of 2% Ba-ZSM-5, 1.5% Ce-ZSM-5, and 1.5% B-ZSM-5 were 82.13%, 81.77%, and 79.84%, respectively. Also, heavy hydrocarbon selectivity of *n_{opt}* % Me-ZSM-5 catalysts was clearly reduced compared to that of the parent catalyst. The 2% Ba-ZSM-5 had a minimum selectivity for ethylene (7.55%) and light paraffins (2.87%) and the highest selectivity of butylene (29.49%) as well as P/E ratio (about 5.97) among *n_{opt}* % Me-ZSM-5 catalysts, corresponding to the hydrocarbon pool mechanism.

In this mechanism, two catalytic hydrocarbon pool cycles were proposed during MTH reaction over the HZSM-5 catalyst: an olefin-based cycle and aromatic-based cycle. The main parts of propylene and higher olefins are produced from methylation/cracking of C₃⁺ alkenes in the olefin-based cycle. On the contrary, the entire ethylene is produced through methylation/dealkylation of poly-methylbenzene as the aromatic intermediate in

the aromatic-based cycle.⁵⁸ Metal-modification of the HZSM-5 catalyst can enhance both the diffusion resistance of the low aromatic intermediate and the residence time in the pore channels of HZSM-5.

The coverage of some strong acid sites with a weak aromatic intermediate prevents the side reactions of propylene and increases the propylene selectivity. It was reported that the alkaline earth metal over the HZSM-5 catalyst led to the suppression of hydrogen transfer reactions in the cracking of n-butane and subsequently reduction of aromatic products.⁵⁹ This finding was in agreement with the reported results of the MTO reaction using the same modified catalyst.⁶⁰ The acidity results show that the number of strong acid sites of 2% Ba-ZSM-5 is drastically reduced compared to that of the HZSM-5 catalyst. Such a reduction in the number of strong acid sites causes a reduction in the amount of active aromatic intermediates, which reduces ethylene production, accelerates the alkene cycle, and increases the propylene selectivity and P/E ratio.⁴²

Despite the reduction in the number of strong acid sites of 2% Mn-ZSM-5, it produces more ethylene than the HZSM-5 catalyst. However, the rapid progress of the alkene cycle compared to the aromatic cycle leads to more increase in propylene selectivity as well as the P/E ratio. It was also reported that ethylene desorption was accelerated due to the position of manganese species on the crystal surface of the ZSM-5 catalyst.⁶¹ In this regard, the increase of ethylene selectivity with respect to the parent catalyst was also shown in the catalyst modified with Ce and B. On the other hand, a modification with metal (or metal oxide) decreased the strength of strong acid sites in the HZSM-5 catalyst and decreased the strong/weak ratio, which are in favor of improving the propylene selectivity.²⁴ The acidity alteration of the impregnated HZSM-5 catalysts is consistent with the results reported in the literature.^{24,26,33}

The alkaline modified catalyst shows a propylene selectivity of about 46.5% with about 85% selectivity of light olefins and about 5.22 P/E ratio. The short diffusion path length in the DZSM-5 catalyst, due to the presence of mesopores, allows easy exit of the reaction products, especially propylene and butylenes, from the active acid sites of zeolite. Accordingly, the equilibrium reaction shifts to propylene and butylene. Hence, a secondary reaction of converting these compounds to undesirable products such as aromatics and heavier alkenes on the acidic site of catalyst was reduced,³⁹ increasing the selectivity to propylene and butylene.

Based on the results of NH₃-TPD analysis, both the weak and strong acid site densities increase with moderate alkaline treatments. It is reported that, weak acidity not only contributes methanol to the DME reaction; it can also participate in the methylation/alkylation reaction cycle and produce light olefins (especially propylene).^{22,23,48} The increase of weak acid site density can improve propylene production and has a positive effect on catalyst stability.⁶² Likewise, the strength of strong acid sites of DZSM-5 decreases relative to HZSM-5, leading to an intensity reduction of secondary reaction performance and conversion decrement of light olefins to precursors of coke.¹⁰ This may be the reason for the DZSM-5 lifetime increment compared to the HZSM-5 catalyst. It should be noted that both weak and strong acid sites are effective in MTP reactions.²⁶ From the point of view of the dual cycle concept, the diffusivity improvement of the desilicated sample causes the residence time of the aromatic intermediates in the active site of zeolite to be reduced, resulting in a decrease in ethylene formation and dramatic enhancement of the olefin-based cycle in the MTP reaction.^{48,63} Therefore, the propylene selectivity and P/E ratio of the alkaline-treated ZSM-5 (DZSM-5) catalysts increased noticeably.

As mentioned earlier, the desilicated ZSM-5 (DZSM-5) catalyst has higher propylene, butylene, and light olefin selectivity compared to the HZSM-5 catalyst. Meanwhile, the heavy hydrocarbon selectivity of DZSM-5 decreased significantly. The heavy hydrocarbon selectivity declined dramatically (<5%) after impregnation of the promoters over the DZSM-5 catalyst.

Meanwhile, it is noteworthy that the propylene selectivity and P/E ratio of HZSM-5 zeolite treated by NaOH solution were 39.8% and 3.37, respectively, as indicated in our previous work.¹⁰ Due to the protective effect of TPA⁺ cations on mesoporosity and crystallinity of the former catalyst to the latter one, the better catalytic performance of the catalyst treated by TPAOH/NaOH compared to the catalyst desilicated with NaOH solution was attributed to better accessibility of the reactants to their active centers.

The selectivities for propylene and light olefins and the P/E ratio in 2% Mn-DZSM-5 as an optimum catalyst were 51.95%, 93.55%, and 5.53, respectively. The selectivities for propylene and light olefins and the P/E ratio in 2% Ba-DZSM-5 were 50.05%, 92.30%, and 6, respectively. The NH₃-TPD results showed that the low strength of strong acidity of 2% Mn-DZSM-5 and 2% Ba-DZSM-5 led to the limited production of heavy hydrocarbons.⁶² The moderate reduction in the density of strong acid sites and appropriate strong/weak acidity ratio after Mn modification over the DZSM-5 catalyst hinder hydrogen transfer reactions and formation of aromatics, thus improving the propylene selectivity compared to 2% Ba-DZSM-5.

It can be concluded that the strong acidity strength reduction, in addition to the decrease in strong/weak acidity, led to more increase in propylene selectivity of n_{opt}% Me-DZSM-5 samples than others. Generally, the n_{opt}% Me-DZSM-5 catalysts represented light olefin (C₂⁻-C₄⁻) selectivity of greater than 90%, which is higher than the values reported in literature.^{8,10,26} It should be noted that the light olefin selectivity over metal/metalloid modified ZSM-5 catalysts (at optimum content) also reached up to 87%. In addition, all the modified catalysts exhibited a noticeably higher selectivity to propylene, butylene, and light olefins than the parent HZSM-5 catalyst while having a relatively lower selectivity toward C₅⁺ hydrocarbons. The comparison between the selectivities of propylene as well as light olefins obtained from the present study and those reported in the literature for MTP reaction are presented in Table 5. As can be seen, with impregnation of 2 wt.% Mn to the DZSM-5 catalyst, the selectivity of both propylene and light olefins improved reasonably.

Table 5. Comparison of propylene and light olefins selectivity obtained from various MTP catalysts reported in the literature.

No	Selectivity of propylene (%)	Selectivity of light olefins (%)	References
1	49.16	–	Zhang et al. ²⁴
2	51	80	Rostamizadeh et al. ⁴⁷
3	55.6	78	Liu et al. ⁸
4	47.2	84.6	Ahmadpour et al. ¹⁰
5	50.1	83	Zhang et al. ²⁷
6	40.04	81.72	Xu et al. ³¹
7	52	93	This work

2.3. Catalyst stability

There is general agreement that coke formation on acid sites (especially strong acid sites) of the MTP catalyst is the main reason for catalyst deactivation.^{8,64} The micropore channels of the HZSM-5 catalyst cause the reaction-produced molecules whose sizes are larger than those of trapped ZSM-5 channels and thereby form a coke precursor. Thus, coke is deposited on the pores and blocks the active acid sites and finally accelerates the catalyst deactivation.^{10,65} As shown in Figure 7, the HZSM-5 catalyst showed a methanol conversion of about

98.5% after 192 h and then reached less than 82% after about 360 h of TOS. Since conversion of less than 90% does not show a good performance for the MTP process in industry, the catalyst must be regenerated or replaced.⁶⁶

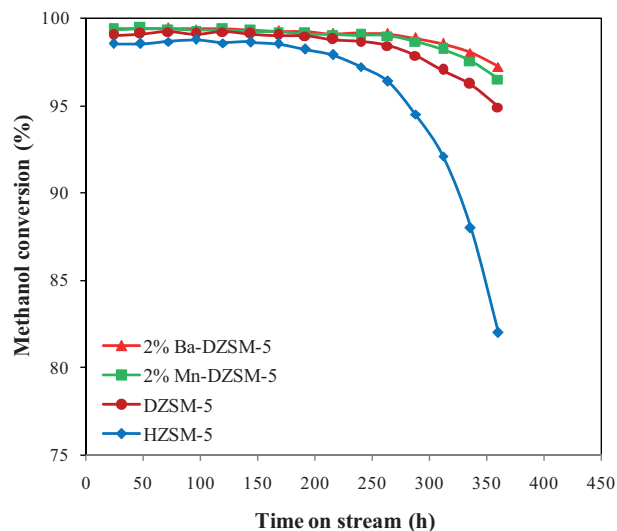


Figure 7. Effect of time on stream on the methanol conversion over HZSM-5, DZSM-5, 2% Mn-DZSM-5, and 2% Ba-DZSM-5 catalysts (reaction conditions: 1 atm, 480 °C, methanol WHSV of 0.9 h⁻¹, methanol/water 1:1 by weight).

As summarized in Table 4, all the modified samples (n_{opt} % Me-ZSM-5, DZSM-5, and n_{opt} % Me-DZSM-5) demonstrated a high conversion after 48 h of TOS (about 99%). High mesoporosity of the DZSM-5 catalyst can improve the diffusion ability of coke precursors and then reduce coke deposition on the zeolite channels. In addition, the reduction in the strength of strong acid sites of the desilicated catalyst is effective in decreasing the formation of the coke precursor, enhancing the catalyst stability.^{10,67} As shown in Figure 7, the DZSM-5 catalyst showed about 99% methanol conversion after 216 h, then dropped slightly to about 95% after 360 h of TOS.

Also, metal impregnation by changing the acid properties of the parent catalyst can be effective on catalyst activity and lifetime.^{26,29} Based on the results of NH₃-TPD analysis, the amount of total acid sites and in particular the amount and strength of strong acid sites were reduced significantly after the impregnation of Mn and Ba promoters, resulting in inhibition of cyclization and hydrogen transfer reactions and thus a reduction in the formation of aromatic intermediates and carbon precursors, which ultimately led to an increase in the stability of these catalysts.^{8,13,24} Based on the NH₃-TPD results, the synergetic reduction of strong acid site strength after HZSM-5 desilication and promoter modification results in the highest stability of the Me-DZSM-5 catalyst. Meanwhile, the coke that formed mainly on the outer surface or mesopores of the Me-DZSM-5 catalyst hindered the pore mouth and active sites of catalyst blockage. Consequently, the stability of mesopore Me-DZSM-5 catalyst is higher than that of the parent catalyst and solo modified catalyst. As can be seen in Figure 7, 2% Mn-DZSM-5 and 2% Ba-DZSM-5 catalysts represent a methanol conversion of about 99% after 264 h, which drops slightly to 96% and 97% after 360 h, respectively. According to Table 3 and Figure 7, the greater stability of 2% Ba-DZSM-5 than 2% Mn-DZSM-5 catalyst can be attributed to less strong acid sites strength/density of the 2% Ba-DZSM-5 than the 2% Mn-DZSM-5 catalyst.

2.3.1. Thermogravimetric analysis (TGA)

The amount of coke deposited on the used catalysts is determined by TGA analysis. Figure 8 shows the resulting TGA curves for the spent parent, DZSM-5, 2% Mn-DZSM-5, and 2% Ba-DZSM-5 samples. These curves represent two distinct weight loss steps. The first weight loss occurring before 350 °C can correspond to desorption of physically adsorbed water, and the second weight loss implied the combustion of carbonaceous species (coke).

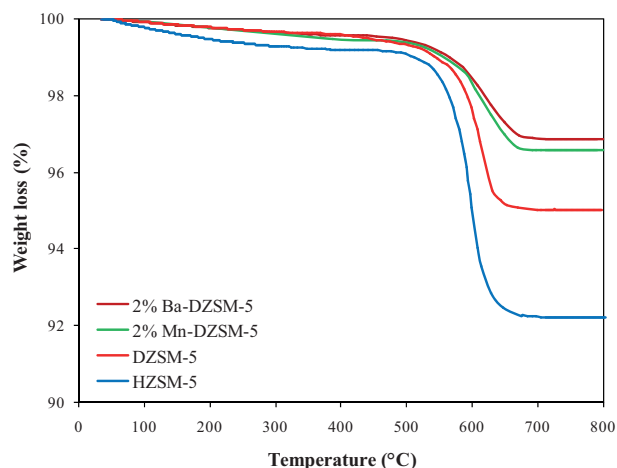


Figure 8. TGA profiles of the spent catalysts (HZSM-5, DZSM-5, 2% Mn-DZSM-5, and 2% Ba-DZSM-5) after undergoing 360 h under the same reaction conditions: 1 atm, 480 °C, methanol WHSV of 0.9 h⁻¹, methanol/water 1:1 by weight.

The amounts of coke deposited for the HZSM-5, DZSM-5, 2% Mn-DZSM-5, and 2% Ba-DZSM-5 samples were 7.02%, 4.60%, 2.97%, and 2.71%, respectively. The average coke formation rates of the HZSM-5, DZSM-5, 2% Mn-DZSM-5, and 2% Ba-DZSM-5 samples were approximately 0.0195, 0.0127, 0.0082, and 0.0075 wt.% h⁻¹, respectively. Therefore, by applying the metal-modified integrated desilicated catalysts, a lower coke formation rate is obtained, accompanied by a longer lifetime than those of the parent and solo desilicated sample.

2.4. Conclusions

In this study, the MTP catalytic performance of high-silica nanostructured HZSM-5 catalyst (Si/Al = 200) modified by metal/metalloid impregnation and alkaline treatment as well as an integrated alkaline metal/metalloid impregnation treatment (impregnated promoters on desilicated catalyst) was investigated in an isothermal fixed bed reactor. The results confirmed that metal impregnation reduced the density and strength of strong acid sites as well as the strong/weak acid sites ratio compared to that of the parent catalyst (unmodified ZSM-5 catalyst). In addition, the alkaline treatment (TPAOH/NaOH) of the HZSM-5 catalyst resulted in the formation of mesoporosity and the reduction of the acid sites strength without significant negative effects on the MFI structure. Also, this modification led to an increment in both strong/weak acid sites density and ratio. A better improvement in the weak acid sites' density and a greater reduction in the strong acid sites' density of the desilicated catalyst after metal impregnation compared to that of the metal-modified parent catalyst led to more decrement of strong/weak acid site ratio without adverse effect on the MFI structure.

Furthermore, the performance of metal-impregnation integrated alkaline treatment in diminishing the strength of strong acidity was more than that of the single modification, due to the synergy effect of combined

treatment. These factors caused controlled side reactions and reduced the byproducts and subsequent improvement of propylene shape selectivity as well as a remarkably prolonged catalytic lifetime. In spite of the fact that methanol was effectively converted to propylene in all the modified samples, impregnation of 2 wt.% Mn over desilicated ZSM-5 catalyst can further improve the selectivity of propylene (about 52%) and light olefins (about 93%) at nearly 99% methanol conversion in the MTP reaction. Moreover, 2% Ba-DZSM-5 catalyst (with about 50% propylene selectivity) showed the best selectivity towards butylene (about 33%) and P/E ratio (about 6) in MTP reaction. The high surface area, the appropriate strong/weak acid site ratio, and the low strength of strong acid sites, in addition to the improved accessibility of the reactants to well-developed mesopore reactive centers, may be the reasons for the best catalytic performance of the 2% Mn-DZSM-5 catalyst.

3. Experimental

3.1. Materials

Tetrapropylammonium hydroxide (TPAOH, 40 wt.% aqueous solution), colloidal silica (Ludox, 40 wt.%), anhydrous sodium aluminate (NaAlO_2 , 55 wt.% Al_2O_3), sodium hydroxide (97 wt.%), ammonium nitrate (95 wt.%), methanol (99.5 wt.%), and ethanol (99 wt.%) were purchased from Merck and were used without further purification. $\text{Mn}(\text{NO}_3)_2 \cdot 4\text{H}_2\text{O}$, $\text{Ce}(\text{NO}_3)_3 \cdot 6\text{H}_2\text{O}$, $\text{Ba}(\text{NO}_3)_2$, and $\text{H}_3(\text{BO}_3)$ were used as the source of promoters from Merck and Sigma-Aldrich.

3.2. Catalyst preparation

3.2.1. Synthesis of parent zeolite

Crystalline HZSM-5 catalyst with Si/Al ratio of 200 was synthesized hydrothermally. The certain amount of NaAlO_2 was added to TPAOH under stirring, and then NaOH was dissolved in distilled water and added to the mixture to give a clear solution. Colloidal silica was added dropwise to the stirred solution to obtain a translucent gel. The gel obtained with a molar ratio of $20 \text{ SiO}_2 : 0.05 \text{ Al}_2\text{O}_3 : 1 \text{ TPAOH} : 1.5 \text{ Na}_2\text{O} : 200 \text{ H}_2\text{O}$.⁵ was stirred for 3 h and then was transferred to a 200-mL Teflon-lined stainless-steel autoclave. Afterward, the autoclave was subjected to hydrothermal treatment at 180 °C for 48 h under autogenous pressure. The zeolite suspension was instantaneously cooled down to room temperature in an ice-water bath to hinder the crystallization. The product was washed several times with distilled water until the pH of the decanted water reached 7, then dried overnight at 110 °C. Finally, the catalyst samples were calcined in a tubular furnace under an air flow at 550 °C for 12 h at a heating rate of 3 °C min^{-1} to eliminate the organic template. After calcination, nanostructured Na-ZSM-5 (sodium form of ZSM-5) was obtained. For ion exchange of Na-ZSM-5, the samples were added into 1 M NH_4NO_3 solution for 12 h at 90 °C under vigorous agitation. This procedure was repeated four times to obtain NH_4 -ZSM-5 zeolite. The samples were then washed with distilled water and dried overnight at 110 °C, followed by calcination at 550 °C for 12 h in an air flow (3 °C min^{-1}) to obtain the H form of ZSM-5. This parent sample was denoted as HZSM-5. The resulting powders were pressed, crushed, and sorted into the size of 18–25 mesh before the catalytic tests.

3.2.2. Alkaline treatment of ZSM-5 zeolite

Alkaline treatment of HZSM-5 zeolite was performed as follows. First, the aqueous solution (90 mL) of a 0.2 M mixture of $\text{NaOH}/\text{TPAOH} = 1.5$.¹⁰ was heated to 65 °C under reflux in an oil bath. Then 3 g of HZSM-5 was put into the heated solution and kept at this temperature while stirring for 30 min; then the slurry was immediately

cooled, washed several times with distilled water, dried, and calcined under the aforementioned conditions. Afterward, the samples were added to 1 M NH_4NO_3 solution for 12 h at 90 °C under vigorous agitation four times. Finally, the sample was washed with distilled water, dried, and calcined under the aforementioned conditions to obtain the H form of desilicated ZSM-5. This sample was denoted as DZSM-5.

3.2.3. Metal/metalloid modification

For the metal/metalloid modification, the wet impregnation method was selected. Different contents (0.5, 1, 1.5, 2, 2.5 wt.%) of Mn, Ce, Ba, and B were loaded on the parent catalyst. In this method, a certain amount of each promoter source (i.e. $\text{Mn}(\text{NO}_3)_2 \cdot 4\text{H}_2\text{O}$) was dissolved in 10 mL of ethanol (for Mn and Ce promoters) or distilled water (for Ba and B promoters). Then 1 g zeolite was added to the above solution while stirring vigorously at ambient temperature for 1 day. The modified catalysts were dried at 110 °C overnight and calcined at 550 °C for 6 h in air (3 °C min^{-1}) and denoted as n% Me-ZSM-5, where n is the concentration (weight percent) of metal/metalloid (Me: Mn, Ce, Ba, B) in zeolite. Then the optimum amount of each promoter ($n_{opt}\%$ Me) on the parent catalyst (based on the maximum selectivity of propylene) was selected for loading on the desilicated catalyst (DZSM-5). The catalysts modified with the above method were denoted as $n_{opt}\%$ Me-DZSM-5. The content of promoter in modified zeolites was calculated by the following relationship:²⁸

$$n = \frac{M_1 z}{m + M_2 z} \times 100, \quad (1)$$

where M_1 and M_2 represent the atomic mass of the metal/metalloid and relative molecular mass of promoter sources, respectively. z is moles of promoters source and m is the mass of zeolite (HZSM-5 or DZSM-5).

3.3. Characterization techniques

Powder X-ray diffraction (XRD) patterns were recorded with an X-pert Pro MPD diffractometer using $\text{Cu K}\alpha$ radiation ($\lambda = 1.5406 \text{ \AA}$) with instrumental settings of 40 kV and 40 mA in the 2θ range of 5–80° with a step size of 0.026. The average crystal size of zeolite samples was estimated by Debye–Scherrer equation from XRD peaks between $2\theta = 7^\circ$ and 10° . XRD was also applied to determine the relative crystallinity of the modified samples. Relative crystallinity was calculated using the integrated peak area method described in ASTM D5758-01.⁶⁸ This calculation is based on a comparison of the integrated peak areas between $2\theta = 22.5^\circ$ and 25° of the modified sample and that of the reference sample (100% of crystallinity was considered for parent HZSM-5 sample).

Elemental analyses were carried out by inductively coupled plasma-optical emission spectroscopy (ICP-OES) using a PerkinElmer Optima 2000 DV. The solution for the ICP-OES analysis was prepared by digesting 0.1 g of ZSM-5 powder in a solution prepared by mixing 1 mL of 36 wt.% HCl, 1 mL of 63 wt.% HNO_3 , 0.5 mL of 50 wt.% HF, and 4 mL of H_2O . After that, HF was neutralized with 2 g of boric acid.

The surface morphology and particle size of the zeolites were examined by field-emission scanning electron microscopy (FE-SEM) conducted on a MIRA3 TE-SCAN microscope. Prior to FE-SEM analysis, the samples were coated with a thin layer of gold. The N_2 adsorption-desorption isotherms and physical properties of the catalysts including surface area and pore volume were evaluated by Brunauer–Emmett–Teller (BET) method on a BELSORP Mini from MicroTrac Bel Corp. The adsorption-desorption isotherms were measured by nitrogen adsorption at -196 °C in a relative pressure range of 0.05–0.99. Prior to measurement, all samples were degassed

under nitrogen flow at 250 °C for about 4 h. The BET equation in the P/P_0 range of 0.05–0.25 was used to calculate the total specific surface area (S_{total}). The total pore volume (V_{total}) was estimated from the nitrogen adsorbed volume at $P/P_0 = 0.99$. The micropore area (S_{micro}) and micropore volume (V_{micro}) were evaluated from the t-plot curve in the P/P_0 range of 0.1–0.4. The mesopore volume (V_{meso}) was estimated from the difference between the V_{total} and V_{micro} .

Fourier transform infrared (FT-IR) analyses of the zeolites were performed to identify surface functional groups with a Spectrum Two (PerkinElmer) instrument.

The acidity of the catalysts was estimated by using temperature programmed desorption of ammonia (NH_3 -TPD) (Micromeritics, ChemiSorb 2750, USA) with an online thermal conductivity detector.

TGA of spent samples, using a Netzsch-TGA 209 F1 instrument, was applied to determine the amount of the coke formed on the catalysts after the stability test. The measurements were performed by scanning the temperature at the heating rate of 10 °C min^{-1} from 30 to 800 °C in an air atmosphere.

3.4. Reactor test

Methanol to propylene reaction was investigated in a fixed bed stainless steel reactor (inner diameter of 9 mm and length of 70 cm) under atmospheric pressure at 480 °C in the catalyst evaluating setup. A schematic flow diagram of the experimental setup is shown in Figure 9. The reactor system was entirely placed in a vertical three-zone tube furnace (PTF 12/75/750, Lenton Ltd., UK). In a typical run, 1 g of meshed catalyst was loaded in the middle section of the isothermal reactor tube. Inert quartz particles (12–16 mesh) were used up and down the catalyst bed to homogenize the gas flow on the catalyst bed and prevent back-mixing. A mixture of

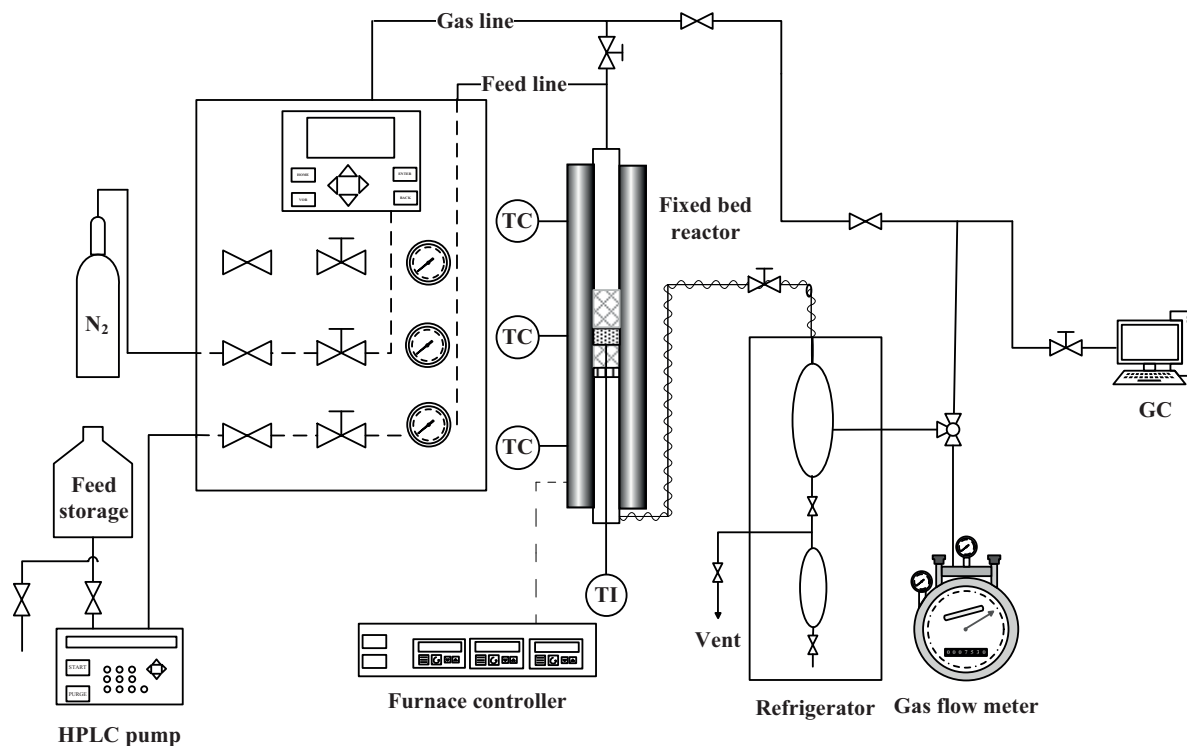


Figure 9. A schematic flow diagram of the lab setup.

50 wt.% methanol in water was pumped with an HPLC pump (Knauer Smartline 1000, Germany) to provide a methanol weight hourly space velocity (WHSV) of 0.9 h^{-1} .

The reactor gaseous products were cooled to 7°C in a refrigerator and the gaseous and liquid products were separated. The gaseous products were analyzed by an online gas chromatograph (GC-Varian 3800) equipped with FID detector and a 50-m HP-PONA capillary column. The liquid products were analyzed offline at the end of the experiments by injecting them into the GC with a Hamilton microsyringe.

Methanol conversion, selectivity, and yield of hydrocarbons were calculated based on the carbon balance.

$$\text{Methanol conversion} = \frac{N_{\text{MeOH}}^i - (N_{\text{MeOH}}^o + 2N_{\text{DME}}^o)}{N_{\text{MeOH}}^i} \times 100 \quad (2)$$

$$\text{Selectivity} = \frac{xN_{\text{C}_x\text{H}_y}^o}{N_{\text{MeOH}}^i - (N_{\text{MeOH}}^o + 2N_{\text{DME}}^o)} \times 100 \quad (3)$$

$$\text{Yield} = \text{methanolconversion} \times \text{selectivity} \quad (4)$$

Here, N is the number of moles and x is the number of carbon atoms. Superscripts i and o represent the components at the inlet and outlet of the reactor, respectively.

In the reactor test, the parent and n% Me-ZSM-5 catalysts with different loading amounts of promoters ($n = 0.5, 1, 1.5, 2, 2.5 \text{ wt.}\%$) were evaluated in MTP reaction to find the optimum amount of each promoter to achieve maximum propylene selectivity. Then the optimum amount of each promoter ($n_{\text{opt}}\%$ Me) was selected for loading on a desilicated catalyst ($n_{\text{opt}}\%$ Me-DZSM-5). Optimum amounts (n_{opt}) obtained for promoters loaded on the parent catalyst were 2, 1.5, 2, and 1.5 wt.% for Mn, Ce, Ba, and B, respectively. In addition, long-term tests were carried out in MTP reactions under the determined conditions over the parent and the selected modified catalysts. Therefore, methanol conversion was recorded as a function of TOS to study the stability of the catalyst.

Acknowledgment

The authors acknowledge the funding support of Babol Noshirvani University of Technology through grant program No. BNUT/370152/97.

References

1. Jiao, Y.; Jiang, C.; Yang, Z.; Liu, J.; Zhang, J. *Microporous Mesoporous Mater.* **2013**, *181*, 201-207.
2. Xiang, D.; Qian, Y.; Man, Y.; Yang, S. *Appl. Energy* **2014**, *113*, 639-647.
3. Baliban, R. C.; Elia, J. A.; Weekman, V.; Floudas, C. A. *Comput. Chem. Eng.* **2012**, *47*, 29-56.
4. Losch, P.; Boltz, M.; Louis, B.; Chavan, S.; Olsbye, U. *Comptes Rendus Chim.* **2015**, *18*, 330-335.
5. Yaripour, F.; Shariatnia, Z.; Sahebdehfar, S.; Irandoukht, A. *J. Nat. Gas Sci. Eng.* **2015**, *22*, 260-269.
6. Plotkin, J. S. *Catal. Today* **2005**, *106*, 10-14.
7. Tian, P.; Wei, Y.; Ye, M.; Liu, Z. *ACS Catal.* **2015**, *5*, 1922-1938.
8. Liu, J.; Zhang, C.; Shen, Z.; Hua, W.; Tang, Y.; Shen, W.; Yue, Y.; Xu, H. *Catal. Commun.* **2009**, *10*, 1506-1509.
9. Wu, W.; Guo, W.; Xiao, W.; Luo, M. *Chem. Eng. Sci.* **2011**, *66*, 4722-4732.
10. Ahmadvour, J.; Taghizadeh, M. *Comptes Rendus Chim.* **2015**, *18*, 834-847.

11. Mei, C.; Wen, P.; Liu, Z.; Wang, Y.; Yang, W.; Xie, Z.; Hua, W.; Gao, Z. *J. Catal.* **2008**, *258*, 243-249.
12. Sun, C.; Du, J.; Liu, J.; Yang, Y.; Ren, N.; Shen, W.; Xu, H.; Tang, Y. *Chem. Commun.* **2010**, *46*, 2671-2673.
13. Ahmadpour, J.; Taghizadeh, M. *J. Nat. Gas Sci. Eng.* **2015**, *23*, 184-194.
14. Schmidt, I.; Boisen, A.; Gustavsson, E.; Ståhl, K.; Pehrson, S.; Dahl, S.; Carlsson, A.; Jacobsen, C. J. H. *Chem. Mater.* **2001**, *13*, 4416-4418.
15. Meng, F. L.; Wang, Z. L.; Zhong, H. X.; Wang, J.; Yan, J. M.; Zhang, X. B. *Adv. Mater.* **2016**, *28*, 7948-7955.
16. Möller, K.; Bein, T. *Chem. Soc. Rev.* **2013**, *42*, 3689-3707.
17. Triantafyllidis, C. S.; Vlessidis, A. G.; Nalbandian, L.; Evmiridis, N. P. *Microporous Mesoporous Mater.* **2001**, *47*, 369-388.
18. Beyer, H. *Post-Synthesis Modif. I.* **2002**, *3*, 203-255.
19. Sadowska, K.; Góra-Marek, K.; Drozdek, M.; Kuśtrowski, P.; Datka, J.; Martínez Triguero, J.; Rey, F. *Microporous Mesoporous Mater.* **2013**, *168*, 195-205.
20. Verboekend, D.; Pérez-Ramírez, J. *Chem. Eur. J.* **2011**, *17*, 1137-1147.
21. Tarach, K.; Góra-Marek, K.; Tekla, J.; Brylewska, K.; Datka, J.; Mlekodaj, K.; Makowski, W.; Igualada López, M. C.; Martínez Triguero, J.; Rey, F. *J. Catal.* **2014**, *312*, 46-57.
22. Yang, Y.; Sun, C.; Du, J.; Yue, Y.; Hua, W.; Zhang, C.; Shen, W.; Xu, H. *Catal. Commun.* **2012**, *24*, 44-47.
23. Xu, A.; Ma, H.; Zhang, H.; Fang, D. *Polish J. Chem. Technol.* **2013**, *15*, 95-101.
24. Zhang, H.; Ning, Z.; Shang, J.; Liu, H.; Han, S.; Qu, W.; Jiang, Y.; Guo, Y. *Microporous Mesoporous Mater.* **2017**, *248*, 173-178.
25. Hadi, N.; Niaei, A.; Nabavi, S. R.; Farzi, A.; Shirazi, M. N. *Chem. Biochem. Eng. Q* **2014**, *28*, 53-63.
26. Rostamizadeh, M.; Taeb, A. *J. Ind. Eng. Chem.* **2015**, *27*, 297-306.
27. Zhang, S.; Zhang, B.; Gao, Z.; Han, Y. *React. Kinet. Mech. Catal.* **2010**, *99*, 447-453.
28. Wang, Y.; Jian, G.; Peng, Z.; Hu, J.; Wang, X.; Duan, W.; Liu, B. *Catal. Commun.* **2015**, *66*, 34-39.
29. Inui, T.; Matsuda, H.; Yamase, O.; Nagata, H.; Fukuda, K.; Ukawa, T.; Miyamoto, A. *J. Catal.* **1986**, *98*, 491-501.
30. Yaripour, F.; Shariatnia, Z.; Sahebdehfar, S.; Irandoukht, A. *Microporous Mesoporous Mater.* **2015**, *203*, 41-53.
31. Xu, A.; Ma, H.; Zhang, H.; Ying, W.; Fang, D. *Int. J. Chem. Mol. Nucl. Mater. Metall. Eng.* **2013**, *7*, 179-184.
32. Ni, Y.; Sun, A.; Wu, X.; Hai, G.; Li, T.; Li, G. *J. Nat. Gas Chem.* **2011**, *20*, 237-242.
33. Ding, J.; Wang, M.; Peng, L.; Xue, N.; Wang, Y.; He, M. *Appl. Catal. A Gen.* **2015**, *503*, 147-155.
34. Groen, J. C.; Peffer, L. A. A.; Moulijn, J. A.; Pérez-Ramírez, J. *Chem. Eur. J.* **2005**, *11*, 4983-4994.
35. Wan, W.; Fu, T.; Qi, R.; Shao, J.; Li, Z. *Ind. Eng. Chem. Res.* **2016**, *55*, 13040-13049.
36. Damjanović, L.; Auroux, A. *Zeolite Chemistry and Catalysis*; Springer: Dordrecht, the Netherlands, 2009.
37. de Rivas, B.; Sampedro, C.; López-Fonseca, R.; Gutiérrez-Ortiz, M.Á.; Gutiérrez-Ortiz, J. I. *Appl Catal A Gen.* **2012**, *417*, 93-101.
38. Chen, L.; Zhu, S. Y.; Wang, Y. M.; He, M. Y. *New J. Chem.* **2010**, *34*, 2328-2334.
39. Bjørgen, M.; Joensen, F.; Spangsbørg Holm, M.; Olsbye, U.; Lillerud, K. P.; Svelle, S. *Appl. Catal. A Gen.* **2008**, *345*, 43-50.
40. Lee, J.; Sohn, K.; Hyeon, T. *J. Am. Chem. Soc.* **2001**, *123*, 5146-5147.
41. Zhuang, J.; Ma, D.; Yang, G.; Yan, Z.; Liu, X.; Liu, X.; Han, X.; Bao, X.; Xie, P.; Liu, Z. *J. Catal.* **2004**, *228*, 234-242.
42. Chen, C.; Zhang, Q.; Meng, Z.; Li, C.; Shan, H. *Appl. Petrochem. Res.* **2015**, *5*, 277-284.

43. Sandoval-Díaz, L. E.; González-Amaya, J. A.; Trujillo, C. A. *Microporous Mesoporous Mater.* **2015**, *215*, 229-243.
44. Gil, B.; Mokrzycki, Ł.; Sulikowski, B.; Olejniczak, Z.; Walas, S. *Catal. Today* **2010**, *152*, 24-32.
45. Campbell, S. M.; Jiang, X. Z.; Howe, R. F. *Microporous Mesoporous Mater.* **1999**, *29*, 91-108.
46. Yu, Q.; Meng, X.; Liu, J.; Li, C.; Cui, Q. *Microporous Mesoporous Mater.* **2013**, *181*, 192-200.
47. Rostamizadeh, M.; Yaripour, F.; Hazrati, H. *J. Anal. Appl. Pyrolysis* **2018**, *132*, 1-10.
48. Zhang, S.; Gong, Y.; Zhang, L.; Liu, Y.; Dou, T.; Xu, J.; Deng, F. *Fuel Process. Technol.* **2015**, *129*, 130-138.
49. Van Laak, A. N. C.; Zhang, L.; Parvulescu, A. N.; Bruijninx, P. C. A.; Weckhuysen, B. M.; De Jong, K. P.; De Jongh, P. E. *Catal. Today* **2011**, *168*, 48-56.
50. Abdelsayed, V.; Shekhawat, D.; Smith, M. W. *Fuel* **2015**, *139*, 401-410.
51. Krishna, K.; Seijger, G. B. F.; van den Bleek, C. M.; Makkee, M.; Calis, H. P. A. *Top. Catal.* **2004**, *30-31*, 115-121.
52. Auroux, A. *Molecular Sieves - Science and Technology*; Springer: Berlin, Germany, 2008.
53. Borry, R. W.; Kim, Y. H.; Huffsmith, A.; Rimer, J. A.; Iglesia, E. *J. Phys. Chem. B* **1999**, *103*, 5787-5796.
54. Kosinov, N.; Coumans, F.; Li, G.; Uslamin, E.; Mezari, B.; Wijpkema, A.; Pidko, E.; Hensen, E. *J. Catal.* **2017**, *346*, 125-133.
55. Liu, W.; Xu, Y.; Wong, S. T.; Wang, L.; Qiu, J.; Yang, N. *J. Mol. Catal. A Chem.* **1997**, *120*, 257-265.
56. Wong, S.; Ngadi, N.; Tuan Abdullah, T. A.; Inuwa, I. M. *Ind. Eng. Chem. Res.* **2016**, *55*, 2543-2555.
57. Van Speybroeck, V.; De Wispelaere, K.; Van der Mynsbrugge, J.; Vandichel, M.; Hemelsoet, K.; Waroquier, M. *Chem. Soc. Rev.* **2014**, *43*, 7326-7357.
58. Svelle, S.; Olsbye, U.; Joensen, F.; Bjørgen, M. *J. Phys. Chem. C* **2007**, *111*, 17981-17984.
59. Wakui, K.; Satoh, K.; Sawada, G.; Shiozawa, K.; Matano, K.; Suzuki, K.; Hayakawa, T.; Yoshimura, Y.; Murata, K.; Mizukami, F. *Catal. Lett.* **2002**, *84*, 259-264.
60. Okado, H.; Shoji, H.; Kawamura, K.; Kohtoku, Y.; Yamazaki, Y.; Sano, T.; Takaya, H. *ChemInform* **1987**, *18*, 25-31.
61. Radu, D.; Glatze, P.; Gloter, A.; Stephan, O.; Weckhuysen, B. M.; De Groot, F. M. F. *J. Phys. Chem. C* **2008**, *112*, 12409-12416.
62. Zhu, Q.; Kondo, J. N.; Ohnuma, R.; Kubota, Y.; Yamaguchi, M.; Tatsumi, T. *Microporous Mesoporous Mater.* **2008**, *112*, 153-161.
63. Wen, M.; Wang, X.; Han, L.; Ding, J.; Sun, Y.; Liu, Y.; Lu, Y. *Microporous Mesoporous Mater.* **2015**, *206*, 8-16.
64. Zhang, J.; Zhang, H.; Yang, X.; Huang, Z.; Cao, W. *J. Nat. Gas Chem.* **2011**, *20*, 266-270.
65. Mole, T.; Whiteside, J. A. *J. Catal.* **1982**, *75*, 284-290.
66. Wang, Y.; Yuan, F. *J. Ind. Eng. Chem.* **2014**, *20*, 1016-1021.
67. Rahmani, M.; Taghizadeh, M. *React. Kinet. Mech. Catal.* **2017**, *122*, 409-432.
68. ASTM International. ASTM Standard Test Method D5758-01. ASTM: West Conshohocken, PA, USA, 2011.